# NUCLEAR INTERACTION DYNAMICS IN $^{56}$Fe(α,xn) REACTION

B.V. Zhuravlev, N.N. Titarenko, V.I. Trykova

State Scientific Center of Russian Federation – Institute for Physics and Power Engineering, 249033 Obninsk, Kaluga Region, Russia

Neutron spectra and angular distributions in $^{56}$Fe(α,xn) reaction have been measured at α-particle energies of 12, 16, 18, 27, 45 MeV. The measurements were performed by time-of-flight fast neutron spectrometers on the pulsed accelerators. The analysis of the measured data have been carried out in the framework of equilibrium, preequilibrium and direct nuclear reaction mechanisms. The calculations are done using the exact formalism of the statistical theory as given by Hauser-Feshbach with the nuclear level densities of Ni isotopes, excited in this reaction, determined on the basis of new experimental data on the low-lying levels, the s-wave neutron resonance spacing and neutron evaporation spectra [1]. The contributions of equilibrium, preequilibrium and direct mechanisms of neutron emission has been studied in a wide energy range of α-particles.

## Introduction

Understanding of the nuclear interaction mechanisms is an overall objective of any nuclear reaction study. In spite of permanent interest to elaboration of fundamental approaches in the description of nuclear interaction in mega-electron-volt range of the energy, the complete understanding of nuclear reaction mechanisms yet it is not achieved. Accordingly the models are not developed, allowing to predict differential cross-sections of interaction with accuracy achievable in experiment. Three types of the interactions described by mechanisms of equilibrium, preequilibrium and direct processes are traditionally distinguished. The equilibrium mechanism of reaction is strictly enough formalized in Hauser-Feshbach model, however big uncertainties arise at modeling of nuclear level density. Analysis of a nonequilibrium part demands more clear split between preequilibrium emission of particles and direct processes, especially one-step, as a rule negligible in the preequilibrium mechanism. Study of the nonequilibrium neutron emission in (α,xn) reaction is represented a little bit easier other reactions with complex particles as in this case the probability of preliminary formation of α-particles is not considered, lack of Coulomb barrier in output channel makes neutron decay predominated one, and the neutron optical potential is most investigated.

In the present work differential cross-sections of $^{56}$Fe(α,xn) reaction are measured at α-particle energies of 12, 16, 18, 27, 45 MeV and analyzed within the framework of equilibrium, preequilibrium and direct mechanisms of interaction. The nuclear level densities of Ni isotopes, excited in this reaction, were determined on the basis of new experimental data on the low-lying levels, the s-wave neutron resonance spacing and neutron evaporation spectra [1].

## Experiment

Spectra and angular distributions of neutrons from $^{56}$Fe(α,xn) reaction are measured at α-particle energies of 12.3, 16.3, 18.3, 26.8, 45,2 MeV. The measurements of neutron spectra were performed by time-of-flight fast neutron spectrometers on the pulsed tandem accelerator at α-particle energies of 12.3, 16.3 and 18.3 MeV in the angle range of $(20\text{-}140)^0$ [2] and on

150 cm cyclotron at α-particle energies of 26.8 and 45.2 MeV in the angle range of $(30\text{-}150)^0$ [3]. As a target were used the self-supporting metal foil with thickness of 0.6 mg/cm$^2$ and 2.6 mg/cm$^2$ and enrichment of 99.5 %. Neutrons were detected by the scintillation detector. For decreasing of the background it was placed in the massive shielding and electronic discrimination of gamma-rays was used. The detector efficiency was determined by measuring of the $^{252}$Cf prompt fission neutron spectrum, yields of monoenergetic neutrons from T(d,n), T(p,n), D(d,n) reactions and direct modeling of interaction of neutrons with organic scintillator. The neutron spectrum measurement procedure has been consisted in measuring with target and without it for the same α-particle flux, registrated by the integrator of a current with Faradey-cup as a charge collector. The background was small in magnitude and practically uncorrelated over time. Typical angle-integrated neutron emission spectra and angular distributions of neutrons from $^{56}$Fe(α,xn) reaction are presented in figs. (1-5). As the α-particle energy increases, a high-energy component manifests itself in the neutron spectra, angular distributions of which are asymmetric, that are a typical indication of nonequilibrium processes in nuclear reactions.

**Data analysis**

For the calculation of an equilibrium part of differential cross-section of reaction we used Hauser-Feshbach mathematical formalism of statistical theory of the nuclear reactions [4], precisely taking into account laws of spin and parity preservation and also the characteristic of low-lying levels of a residual nucleus.

$$\frac{d^2\sigma(E_0,E_2,\theta)}{dE_2 d\Omega}=\frac{1}{4K_0^2}\cdot\sum_{kJ_1}\sum_{l_0 j_0 l_2 j_2}\frac{2J_1+1}{(2S_0+1)\cdot(2J_0+1)}\cdot B_k(l_0,S_0,j_0,J_0,J_1)\cdot\sum B_k(l_2,j_2,S_2,J_2,J_1)\times \\ \times\tau\cdot\rho(E_0+Q_{\alpha,n}-E_2,J_2)\cdot P_k(\cos\theta), \quad (1)$$

$$\tau = \frac{T_{l_0 j_0}(E_0)\cdot T_{l_2 j_2}(E_2)}{\sum_c\left(\sum_{l,j}T_{l,j}+\sum_{l,j,J}\int_{U_c}T_{l,j}\cdot\rho(E_0+Q_{\alpha,n}-E_2,J_2)\cdot dU\right.} \quad (2)$$

$$B_k(l,S,j,J_f,J_i)=(-1)^{J_f-J_i-S}\cdot(2J_i+1)\cdot(2j+1)\cdot\langle l_0 l_0|K_0\rangle W(J_i J_i jj;KJ_f)\cdot W(jjll;KS), \quad (3)$$

where: $\langle l_0 l_0|K_0\rangle$ - Clebsch-Gordan coefficients, $W(J_i J_i jj;KJ_f)$ – Racah coefficients, $P_k(\cos\theta)$ –Legendre polynomials, $K_0$ – wave vector of particle, $l_0,l_2,j_0,j_2,J_0,J_2,E_0,E_2$ – accordingly the orbital moments, spins of particles and nuclei, energy of particles in input and output channels, $J_1$ – spin of compound nucleus, $T_{lj}$ – transmission coefficients, $\rho(E_0+Q_{\alpha,n}-E_2,J_2)$ – nuclear level density, $U = E_0+Q_{\alpha,n}-E_2$ - excitation energy of residual nucleus.

Initial distribution of a compound nucleus on energy and angular moment is determined on the basis of optical model. Then distribution on energy and moment for a residual nucleus is calculated. For each kind of decay and all possible values of energy and moment relative probabilities of emission are calculated and on initial population and relative probability of emission particle emission spectra are determined. After probabilities of the parent nucleus decay are calculated, the obtained distribution of an affiliated nucleus becomes initial on the next step of decay. Spectra of the particles emited at equilibrium decay of a compound nucleus substantially are determined by level density of the residual nuclei excited in researched reaction. Therefore in calculations we used the data on level density of $^{60}$Ni, $^{59}$Ni, $^{58}$Ni and $^{57}$Ni determined on the basis of new experimental data on the low-lying levels, the neutron resonance spacing and neutron evaporation spectra [1]. Fig. 6 shows the level density of $^{59}$Ni nucleus excited at the first step of neutron emission in $^{56}$Fe(α,xn) reaction.

One can see that the description of the experimental data in the framework of the different model systematics differs markedly.

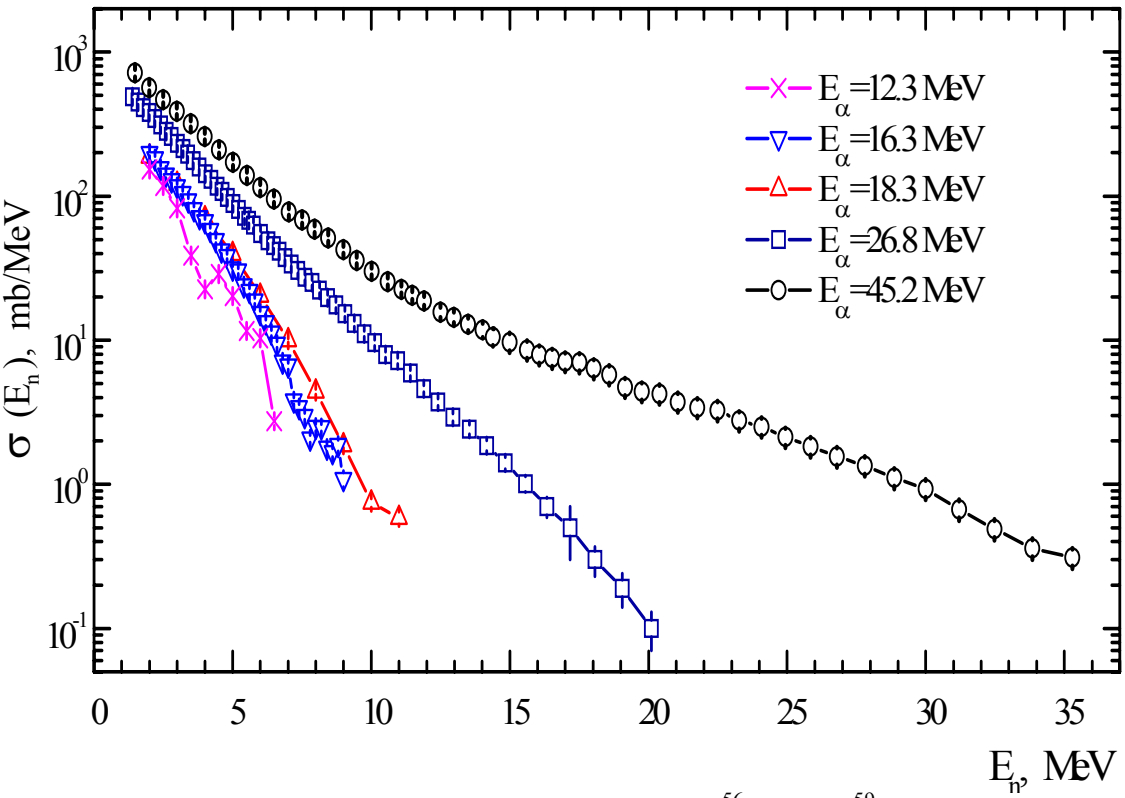


**Fig.1.** Angle-integrated neutron spectra from $^{56}Fe(\alpha,xn)^{59}Ni$ reaction.

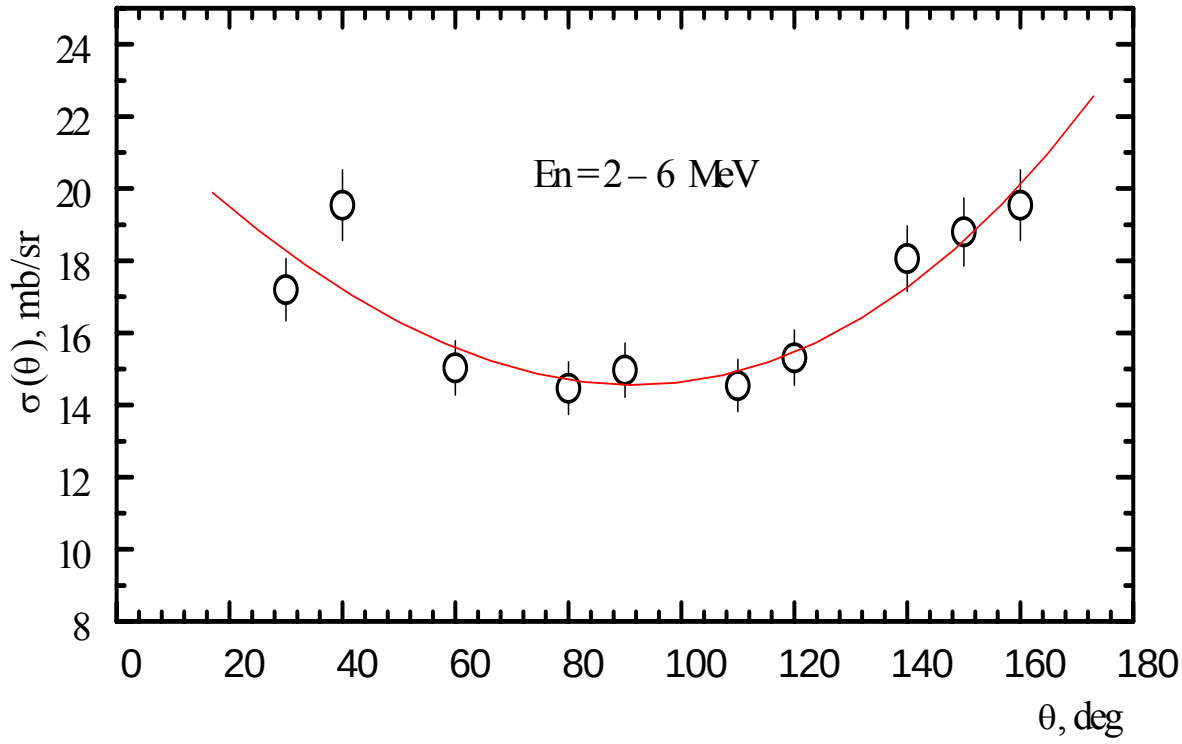


**Fig.2.** Angular distribution of neutrons from $^{56}Fe(\alpha,n)^{59}Ni$ reaction at $E_a$ =12,3 MeV. Curve - approximation data by Legendre polynomials.

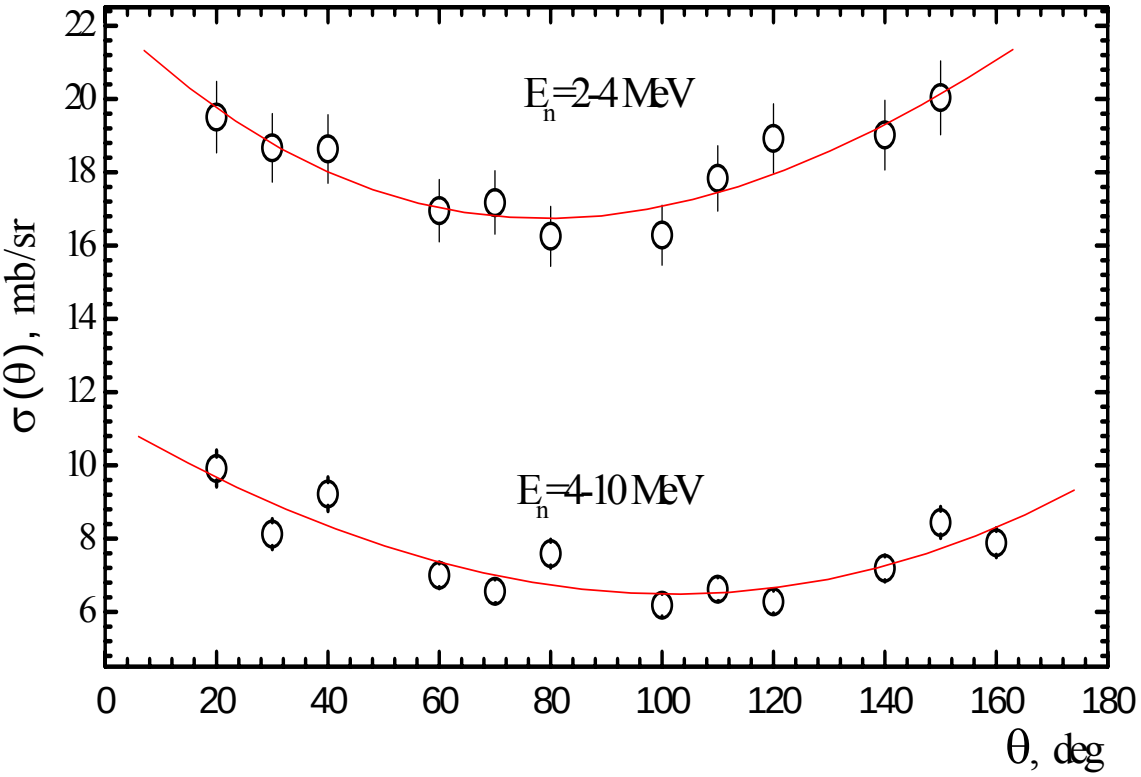


**Fig.3.** Angular distribution of neutrons from $^{56}Fe(\alpha,n)^{59}Ni$ reaction at $E_a$ =16,3 MeV. Curve - approximation data by Legendre polynomials.

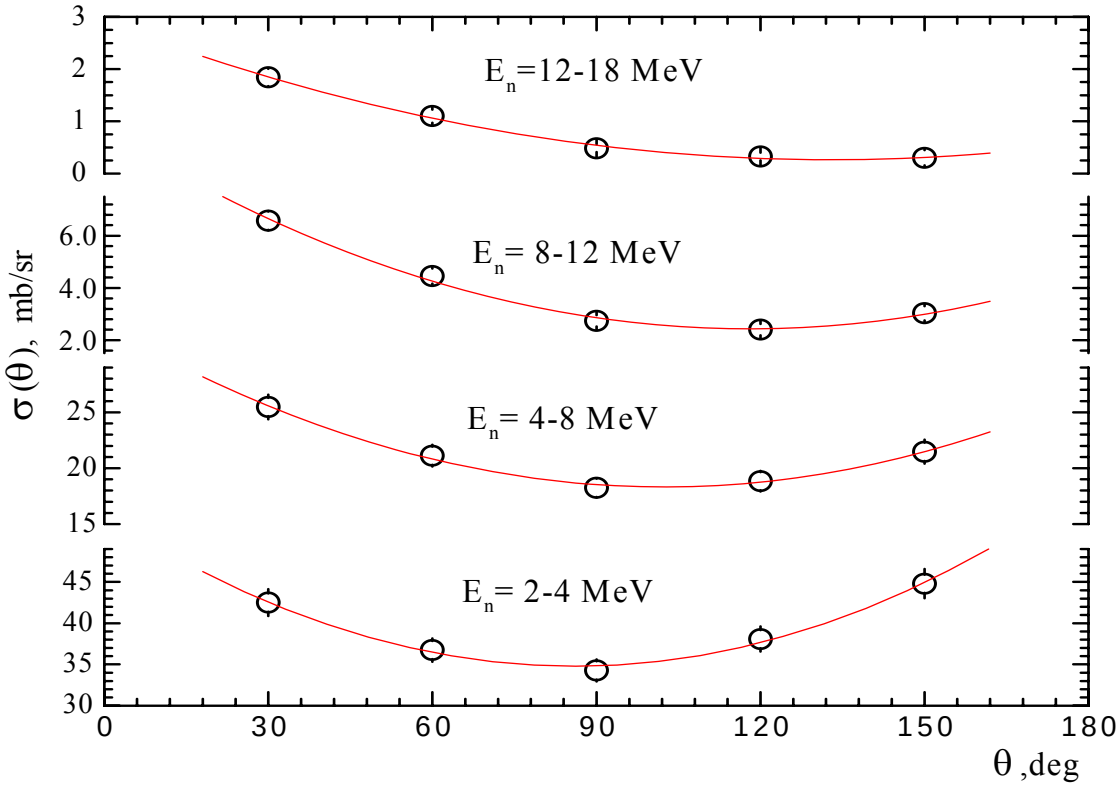


**Fig.4.** Angular distribution of neutrons from $^{56}Fe\ (\alpha,xn)^{59}Ni$ reaction at $E_a$ =26.8 MeV. Curve - approximation data by Legendre polynomials.

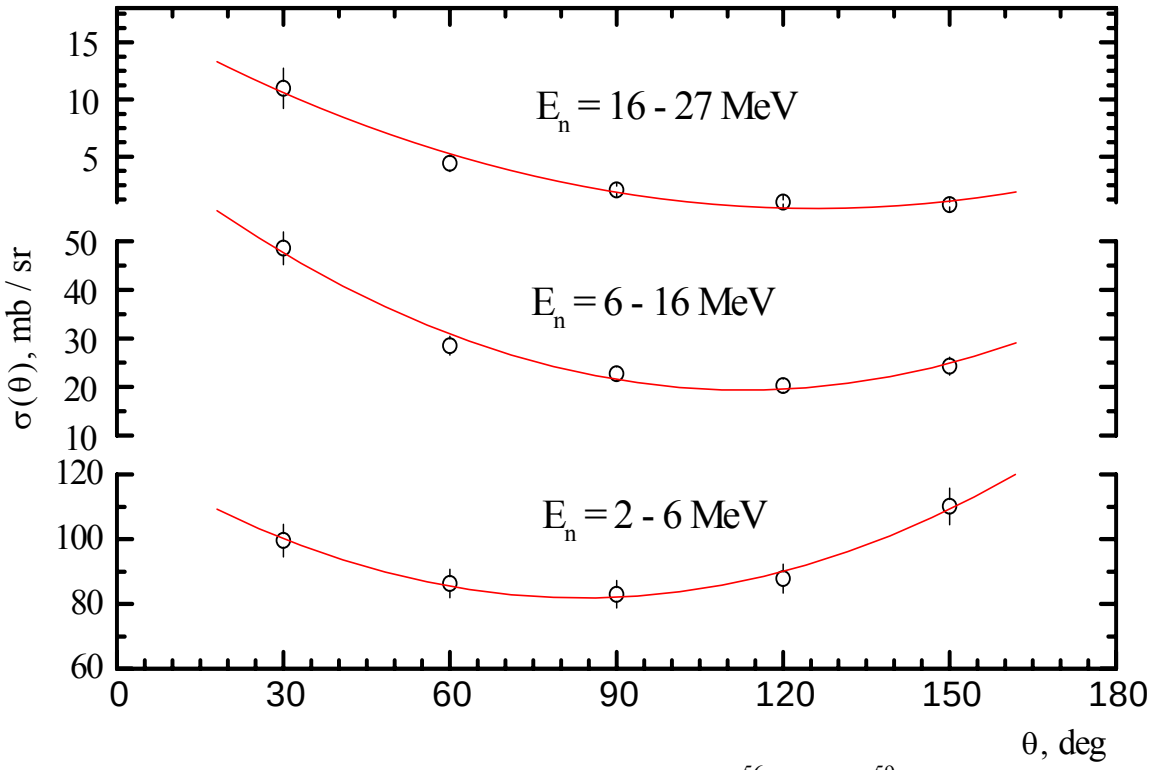


**Fig.5.** Angular distribution of neutrons from $^{56}Fe(\alpha,xn)^{59}Ni$ reaction at $E_a$ =45.2 MeV. Curve - approximation data by Legendre polynomials.

Calculations of preequilibrium neutron emission are executed in the framework of exciton model [5,6].

$$\frac{d\sigma(E_n)}{dE_n} = \sigma_a(E_o)\cdot\sum_{n=n_o}^{n_{max}}\lambda(n,E_n)\cdot\tau(n,E\ ), \qquad (4)$$

$$\lambda(n,E_n) = \frac{2s+1}{\pi^2\cdot\hbar^3}\cdot\mu\cdot E_n\cdot\sigma_c(E_n)\cdot R\cdot\frac{\omega(p-1,h,U)}{\omega(p,h,E\ )}, \qquad (5)$$

$$\omega(p,h,E) = \frac{g\cdot(g\cdot E - A_{p,h})^{n-1}}{p!\cdot h!\cdot(n-1)!}, \qquad (6)$$

where: s, μ, En - spin, reduced mass and neutron energy,

g - single particle state density (g=A/13),

$\sigma_\alpha(E_0)$ - absorption cross-section of α-particles by nucleus,

$\sigma_c(E_n)$ - inverse reaction cross-section,

E and U - excitation energy, respectively, for composite and residual nuclei,

n=p+h - exciton number of the system (p - particles, h - holes),

τ(n,E) - mean life-time of composite nucleus in n-exciton state,

R - factor, which is taking into account distinction of neutrons and protons in the internuclear cascade, was calculated in the assumption that in each pair interaction the proton and neutron are created with relative probabilities Z/A and N/A.

$A_{p,h}$ - Pauli correction function.

In calculations are taken into account surface, shell structure and pairing effects. The initial exciton number "$n_o$" is a parameter of model and we used a configuration 4p0h ($n_o$=4) in the assumption, that all α-particles collapse on nucleons in a field of a nucleus-target. The quantity of the square of the average matrix element in model was 135.6 $MeV^2$.

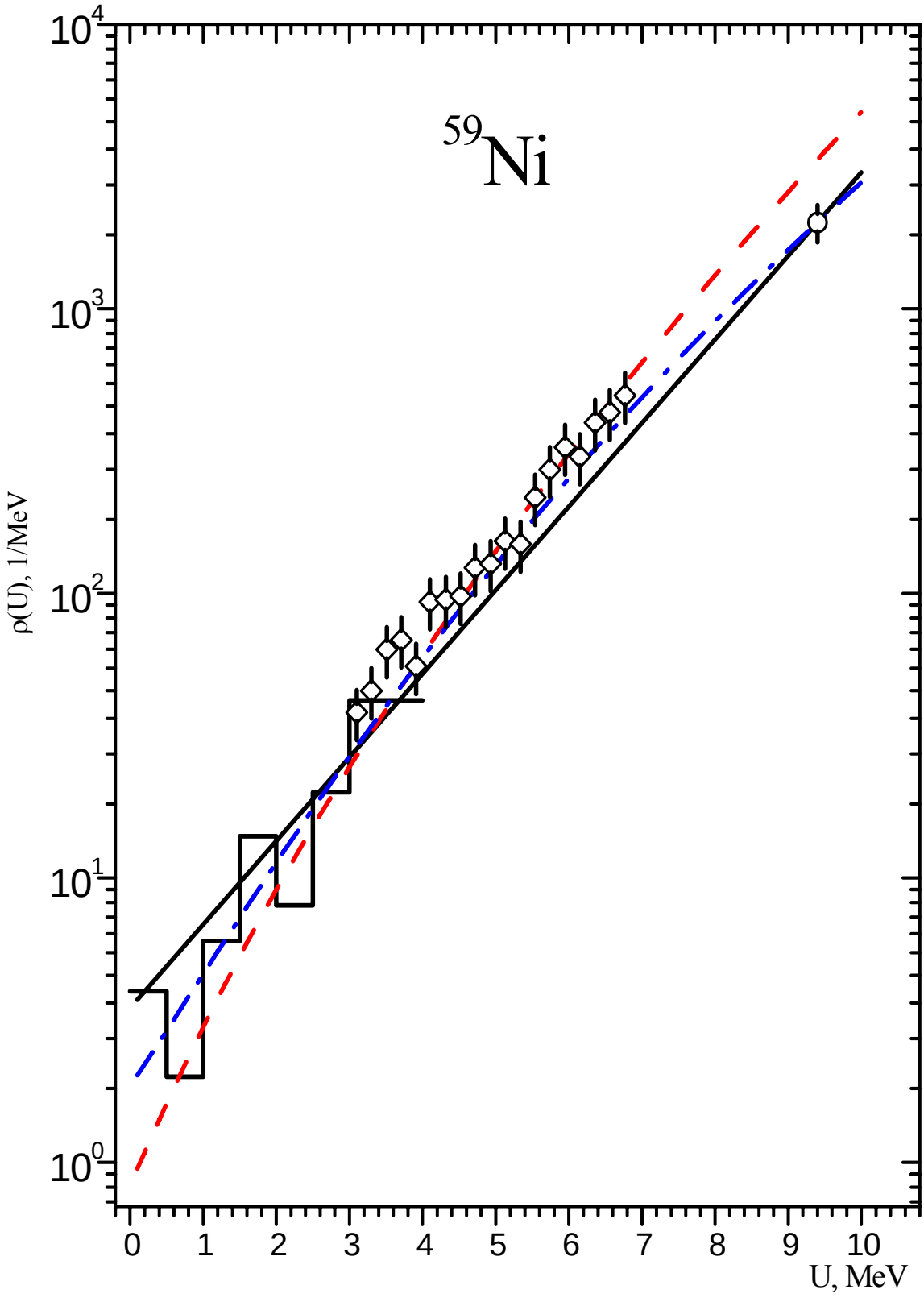


**Fig. 6.** Nuclear level density of the $^{59}$Ni. ◊ - data obtained in our study from neutron evaporation spectra in $^{59}$Co(p,n)$^{59}$Ni reaction [1], histogram – low-lying level data , o - neutron resonance data. Curves are results of the calculations: dash-dotted - on the generalized model of a superfluid nucleus, dashed - on the back-shifted Fermi-gas model, solid - on the Gilbert–Cameron composite formula.

All calculations within the framework of optical-statistical models of equilibrium and preequilibrium decay of nucleus are carried out on modernized GNASH code [7], allowing to trace the decay of the excited compound nucleus with account of the emission of neutrons, protons, α-particles and γ-quantums. For neutrons and protons the optical potential from work [8], for α-particles - from work [9] and for deuterons - from work [10] was used.

For the full calculation of particle emission in nuclear reaction the separate direct interactions it is necessary to consider in addition to exciton model of preequilibrium emission [11]. At consideration of direct interaction effects it is important to know, what kinds of direct processes are taken into account in the framework of exciton model and to find independent ways of calculation of direct interactions which are not taken into account. In our case process of direct stripping of three nucleons of α-particle and direct knockout process of neutron by α-particle are not taken into account in the considered variant of exciton model, in which the initial stage of preequilibrium emission is ($n_o$=4, p=4, h=0), when α-particle collapses on four nucleons in the field of a nucleus-target.

The general differential cross-section formula for continuum stripping reaction $^{56}$Fe(α,n)$^{59}$Ni is [11]

$$\frac{d\sigma(E_n)}{dE_n} = \frac{2s_n+1}{2s_\alpha+1}\cdot\frac{A_n}{A_\alpha}\cdot\frac{E_n\cdot\sigma_c(E_n)}{A_\alpha\cdot E_\alpha}\cdot K\cdot\left(\frac{A_\alpha}{E_\alpha+V_\alpha}\right)^{2n}\cdot\left(\frac{C}{A_{Ni}}\right)^{n}\cdot 0.0127\cdot\omega(p,h,U), \quad (7)$$

where: $s_n$ , $s_\alpha$ - spins of neutron and α-particle,
$A_n$ , $A_\alpha$ , $A_{Ni}$ - mass number of neutron, α-particle and residual nucleus $^{59}$Ni,
$E_\alpha$ - α-particle energy,
$V_\alpha$ - well depth ($V_\alpha$=12.5$A_\alpha$=50 MeV),
n - exiton number, n=$A_\alpha$-$A_n$=3 (p=3, h=0),
ω(p,h,U) - accesible state density given by Eq (6).

The total residual state density however also takes into account more complex configurations that can be excited by stripping reaction [11].

Direct knock-out process of neutron by α-particle also is not taken into account in the considered variant of exciton model. For the account of this mechanism we considered an α-particle as cluster, exciting a neutron particle-hole pair in a nucleus-target ($n_o$=3, p=2, h=1), by analogy to how it is realized in works [11,12]. The differential cross-section for continuum knockout reaction is

$$d\sigma(E_n)/dE_n = const\cdot(2s_n+1)\cdot\mu\cdot E_n\cdot\sigma_c(E_n)\cdot g_n\cdot g_\alpha\cdot(U-1/2g_n-1/2g_\alpha), \quad (8)$$

where: $g_n$=N/13, $g_\alpha$=A/208, the normalizing multiplier "const" was determined from the best fit of calculation and experimental data in a high-energy part of neutron spectra.
The cross-section of direct neutron sripping and knock-out processes are calculated separatly and cross-section of preequilibrium emission is overnormalized on their quantity.

## Results

The tipical calculated according to the procedure described above neutron spectra from $^{56}$Fe(α,xn) reaction at all investigated values of α-particle energy are shown in figs.(7 - 11). The calculated and measured angle-integrated neutron spectra are in agreement as a whole within the limits of errors of measurements. In the table integrated cross-sections of equilibrium, preequilibrium, stripping, knock-out neutron emission and total cross-sections of reaction are presented also.

**Table.** Cross-sections of equilibrium, preequilibrium, stripping, knock-out neutron emission and total neutron emission cross-sections of $^{56}$Fe(α,xn) reaction.

| Eα, MeV | σ equil., mb | σ preeq., mb | σ strip., mb | σ knock., mb | σ total, mb |
|---|---|---|---|---|---|
| 12.3 | 465 | 16 | - | - | 481 |
| 16.3 | 606 | 45 | - | - | 651 |
| 18.3 | 685 | 49 | - | - | 734 |
| 26.8 | 1443 | 77 | 49 | 39 | 1608 |
| 45.2 | 1994 | 249 | 54 | 25 | 2322 |

One can see that the neutron emission spectra from $^{56}$Fe(α,n)$^{59}$Ni reaction at α-particle energies of 12.3, 16.3 and 18.3 MeV mainly are caused by the equilibrium neutron emission; contributions of the preequilibrium neutron emission are small (3-7%) and, practically, have not influence on the shape of the neutron spectra. At higher α-particle energies ($E_\alpha$=26.8 and 45.2 MeV) the hard part of the angle-integrated neutron spectra ($E_n \geq 15$ MeV) are associated, mainly, with nonequilibrium emission of neutrons and as, one can see from figs. 10 and 11, taking into account of the direct interaction processes (stripping and knock-out) allows reliably to describe the experinental data at these values of α-particle energies both in the hard parts of the spectra and in the entire energy range of emitted neutrons. Though the cross-sections of the stripping and knock-out processes at α-particle energy of 45.2 MeV put together about 3.5 % from total neutron emission cross-section, the hard part of the observed neutron spectrum with $E_n \geq 25$ MeV can be described only if these direct processes are taken into account in nuclear reaction mechanisms.

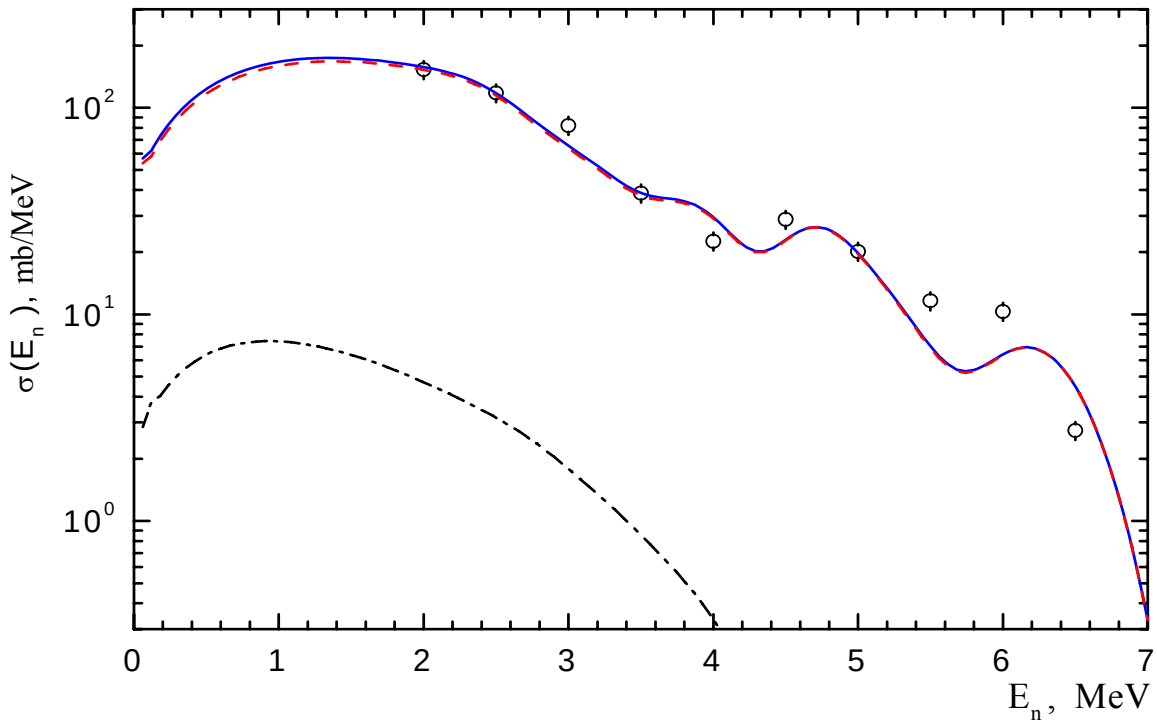


**Fig.7.** Neutron spectra from $^{56}$Fe (α,n )$^{59}$Ni reaction at $E_\alpha$ =12.3 MeV. o –experiment, curves - calculation: ———— - summary contribution: — — — - equilibrium emission, —·—·— - preequilibrium emission .

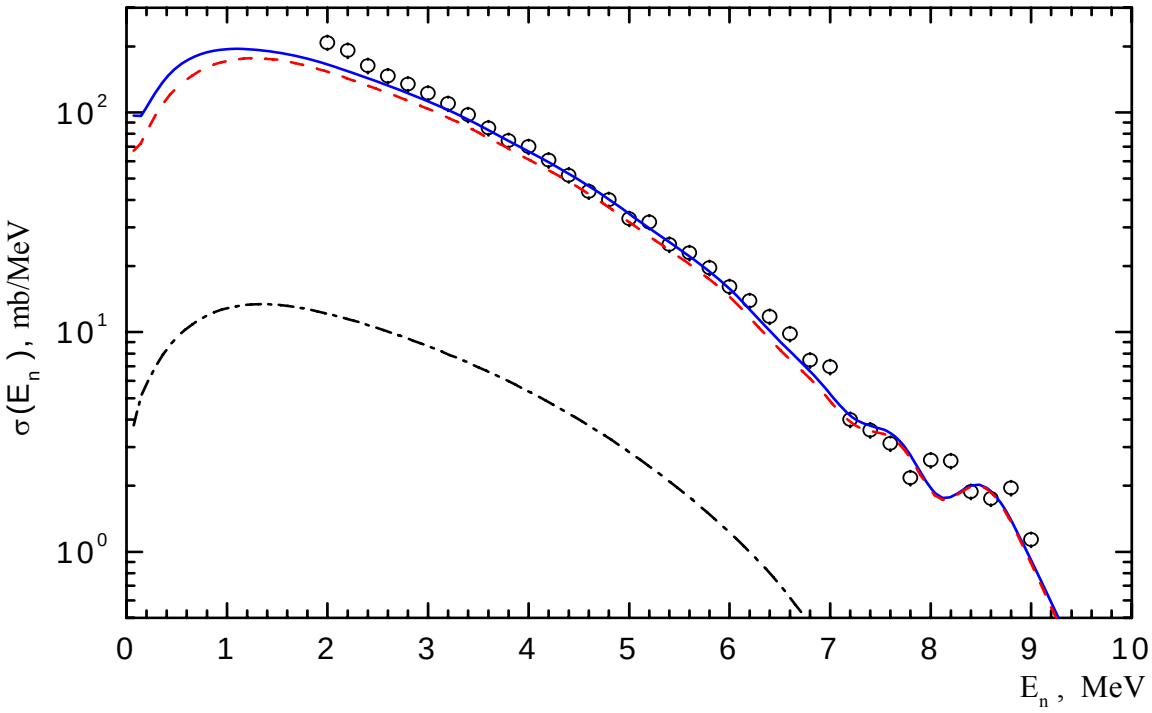


**Fig. 8.** Neutron spectra from $^{56}$Fe(α,n)$^{59}$Ni reaction at $E_\alpha$ =16.3 MeV. Designations are the same as in Fig. 7.

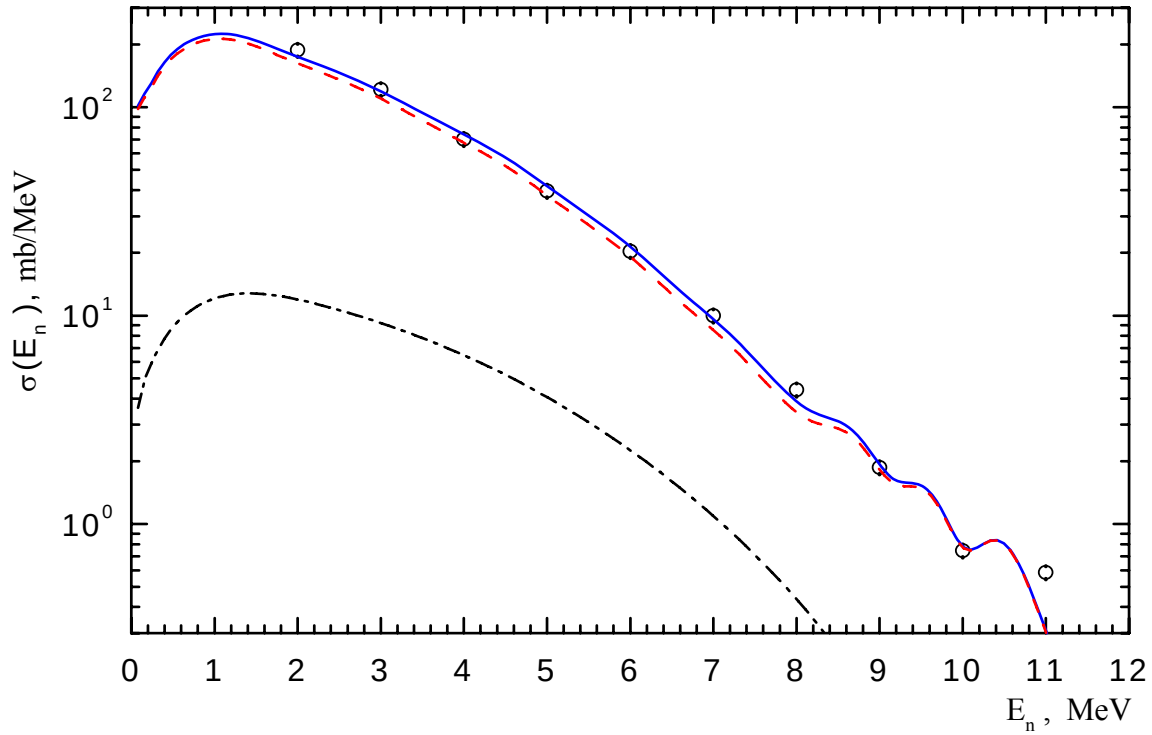


**Fig.9.** Neutron spectra from $^{56}$Fe (α,n)$^{59}$Ni reaction at $E_\alpha$ = 18.3 MeV. Designations are the same as in Fig. 7.

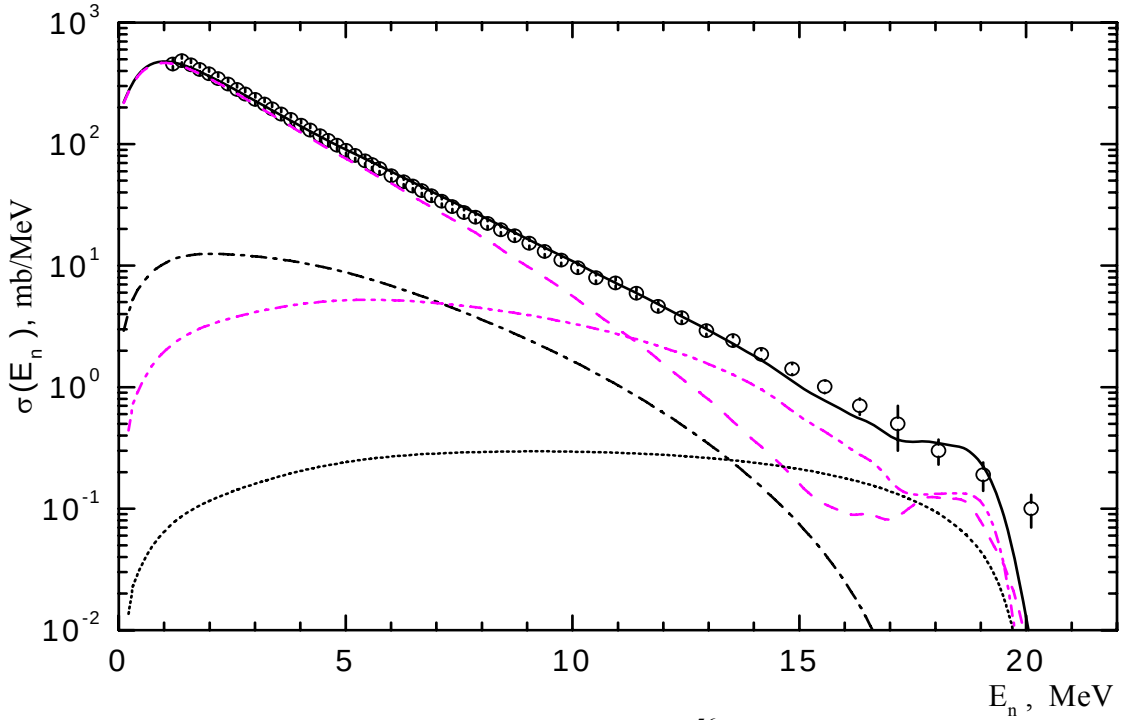


**Fig.10.** Neutron spectra from reaction $^{56}$Fe(α,xn) at $E_\alpha$ =26.8 MeV. o –experiment, curves - calculation: ———— - summary contribution, — — — equilibrium emission, —·—·— - preequilibrium emission, —··—·· — - stripping reaction, ·····  - knock-out reaction.

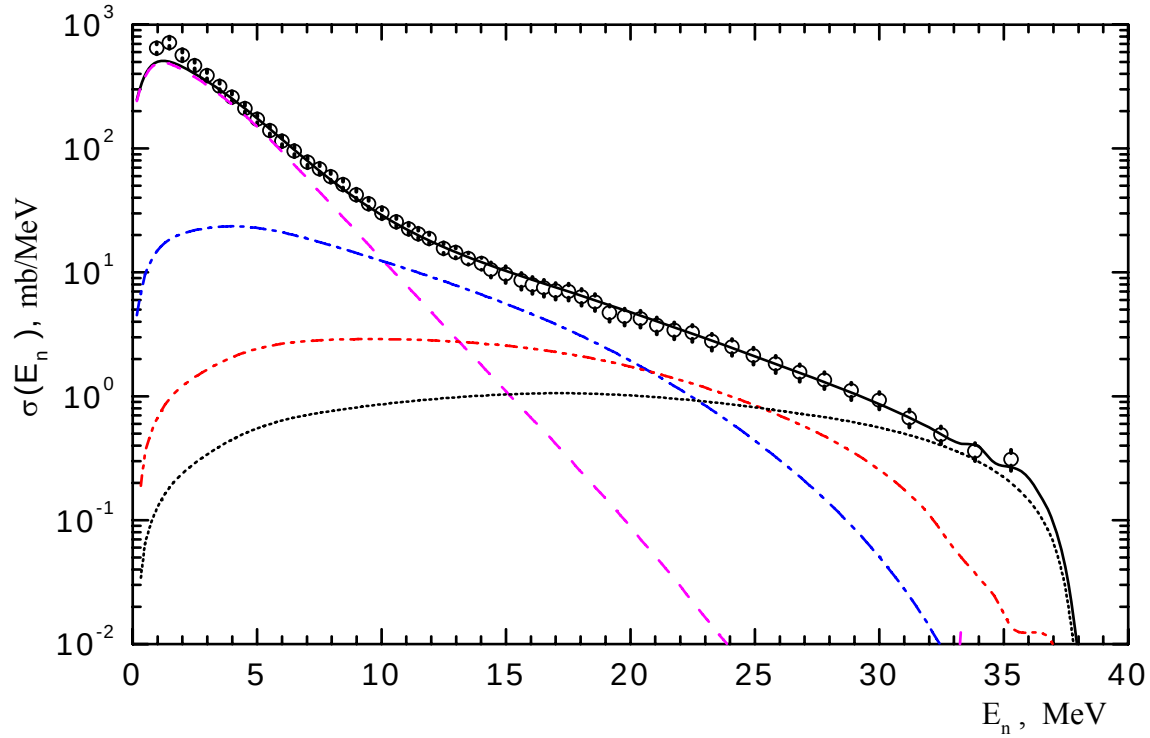


**Fig.11.** Neutron spectra from reaction $^{56}$Fe(α,xn) at $E_\alpha$ =45.2 MeV. Designations are the same as in Fig. 10.

## Conclusion

The differential neutron emission cross-sections in $^{56}Fe(\alpha,xn)$ reaction are measured at α-particle energies of 12.3, 16.3, 18.3, 26.8, 45.2 MeV and are analysed within the framework of equilibrium, preequilibrium, direct stripping and knock-out mechanisms of the particle emission in nuclear reactions. The spectra of all four mechanisms of neutron emission are calculated and is shown, that the calculation results are in an agreement with the measured neutron spectra within the limits of measurement errors. Use of the new experimental data on the nuclear level density of $^{59}Ni$, excited on a first step of neutron emission in $^{56}Fe(\alpha,xn)$ reaction, has allowed reliably to determine the contribution of equilibrium emission. Cross-sections of equilibrium, preequilibrium, direct stripping and knock-out neutron emission in reaction are determined at all investigated values of α-particle energies. It is shown, that the cross-section of nonequilibrium emission is essentially increased with growth of α-particle energy and at α-particle energy of 45.2 MeV the hard part of the observed neutron spectrum with $E_n > 15$ MeV is associated mainly with nonequilibrium emission of neutrons.

This work has been supported in part by the Russian Foundation for Basic Researches and Kaluga Scientific Center (grant 07-02-96400).

**References**:

1. Zhuravlev B.V., Lychagin A.A., Titarenko N.N., Demenkov V.G., Trykova V.I., Grigoriev Yu.V., Doroshenko A.Yu. "Nuclear level densities of nickel isotopes". In *Proceedings of Region Competition of Scientific Projects in Natural Sciences, Kaluga Scientific Center, in print.*
2. Zhuravlev B.V., Titarenko N.N., Trykova V.I. et al. Izv. AN, ser. fizicheskaya, 1999, v.63, №5, p. 959-967.
3. Zhuravlev B.V.., Dovbenko A.G. Yadernaya Fizika, 1995, v.58(10), p.1731-1734.
4. Hauser W., Feshbach H. Phys. Rev., 1952, v.87, p.366
5. Zhivopiszev F.A., Kebin E.I., Sukharevskij V.G. "Models of preequilibrium nuclear reactions", Moscow State University, 1987, p. 31
6. Kalbach C. Zeitschrift fur Physik A, 1977, v. 283, p. 401-411.
7. P.G. Young, E.D. Arthur and M.B. Chadwick, in *Proceedings of IAEA Workshop on Nuclear Reaction Data and Nuclear Reactors, Trieste, Italy, April 15 - May 17, 1996* (World Sci., Singapore, 1998), Vol.1, p.227
8. Koning A.J. and Delaroche J.D. Nucl. Phys. A, 2003, v. 713, p. 231.
9. Avrigeanu V., Hodgson P.E., Avrigeanu M. Phys. Rev. C, 1994, v.49, p. 2255.
10. Daehnick W.W., Childs J.D., Vrecelj Z. Phys. Rev. C, 1980, v. 21, p.2253.
11. Kalbach C. Users manual for PRECO-2000. Duke University, 2001, retrived from www.nndc.bnl.gov/nndcscr/model-codes/preco-2000/.
12. Biryukov N.S., Zhuravlev B.V. et al. Yadernaya Fizika, 1977, v.25(4), p.767-771.